Specific Isoforms of Actin-binding Proteins on Distinct Populations of Golgi-derived Vesicles*

Kirsten Heimann‡, Justin M. Percival§, Ron Weinberger§, Peter Gunning§¶, and Jennifer L. Stow‡‖

From the ‡Centre for Molecular and Cellular Biology, University of Queensland, Brisbane, Queensland 4072 and the §Oncology Research Unit, The New Children's Hospital, Westmead, and Department of Paediatrics and Child Health, University of Sydney, Sydney, New South Wales 2145, Australia

Golgi membranes and Golgi-derived vesicles are associated with multiple cytoskeletal proteins and motors, the diversity and distribution of which have not yet been defined. Carrier vesicles were separated from Golgi membranes, using an *in vitro* budding assay, and different populations of vesicles were separated using sucrose density gradients. Three main populations of vesicles labeled with β-COP, γ-adaptin, or p200/myosin II were separated and analyzed for the presence of actin/actin-binding proteins. β-Actin was bound to Golgi cisternae and to all populations of newly budded vesicles. Centractin was selectively associated with vesicles co-distributing with β-COP-vesicles, while p200/myosin II (non-muscle myosin IIA) and non-muscle myosin IIB were found on different vesicle populations. Isoforms of the Tm5 tropomyosins were found on selected Golgi-derived vesicles, while other Tm isoforms did not colocalize with Tm5 indicating the association of specialized actin filaments with Golgi-derived vesicles. Golgi-derived vesicles were shown to bind to F-actin polymerized from cytosol with Jasplakinolide. Thus, newly budded, coated vesicles derived from Golgi membranes can bind to actin and are customized for differential interactions with microfilaments by the presence of selective arrays of actin-binding proteins.

Protein trafficking into and out of the Golgi complex requires multiple populations of membrane-bound vesicles or tubules. Each vesicle population is associated with distinct sets of coat complexes, G proteins, and SNARE proteins designed to ensure the selective trafficking of cargo proteins. The Golgi complex is also associated with diverse cytoskeletal elements, and Golgi-derived vesicles must, it now appears, carry multiple molecular motors in order to interact with different cytoskeletal structures (1, 2). Microtubules and microtubule-based motors participate in positioning of the Golgi complex within the cell and in vesicular transport between the endoplasmic reticulum and Golgi as well as in some post-Golgi pathways (3). Elements of the actin cytoskeleton are also involved in Golgi trafficking. The p200/myosin II protein, analogous to the heavy chain of nonmuscle myosin IIA, binds specifically to vesicles budding off

the trans-Golgi network (TGN)[1] in many cells (4–7). Brush border myosin I has been localized to Golgi membranes, vesicles, and secretory granules (8–11). Dynactin and myosin I are found on the same carrier vesicles budding off the TGN in epithelial cells (11). Myosin 5a can interact with actin as well as with microtubules (12), and diverse roles, ranging from synaptic vesicle transport (13) to the movement of smooth endoplasmic reticulum and pigment granules, have been proposed for myosin 5a (14). Recent studies show that some isoforms of cytoskeletal proteins associate uniquely with the Golgi, suggesting that the Golgi has its own, dedicated cytoskeleton. A Golgi-specific kinesin-like protein (Rab-kinesin; Ref. 15), a Golgi-specific isoform of spectrin (16), and two isoforms of ankyrin that are concentrated on the Golgi complex (17, 18) have been identified.

The potential roles of actin filaments and their associated proteins in either maintaining Golgi structure or in vesicular trafficking are not well understood. In most cells the Golgi complex is closely aligned with the microtubule-organizing center, but such a morphologically distinct, stable connection to the Golgi complex is not evident for microfilaments. The association of actin and actin-binding proteins with Golgi membranes might therefore be more dynamic. The use of actin-polymerizing or -depolymerizing drugs has served to generally implicate the actin cytoskeleton in vesicular trafficking, especially in endocytic pathways in intact cells (19, 20). Secretory yeast mutants have provided the most direct evidence for a requirement for actin in vesicular transport. The temperature-sensitive mutant of Myo2p, a myosin V gene product of the yeast *Saccharomyces cerevisiae*, has defective post-Golgi transport and accumulates vesicles destined for the vacuole and for exocytosis (21–25). Mutation of the Act-1 genes in yeast block secretion (26). These studies demonstrate that the actin cytoskeleton, at some level, does participate in vesicle trafficking, but specific roles for actin in various stages of vesicle budding, transport, or targeting remain unknown.

Proteins participating in vesicular transport interact with highly specific membrane domains, either on cisternal membranes in different parts of the Golgi stack or on selected vesicles. The distribution of individual proteins thus often indicates their sites of action in different pathways or steps of vesicle transport. The current study was undertaken to determine the distributions of actin and actin-associated proteins with Golgi membranes and with Golgi-derived vesicles. Using an *in vitro* assay to generate different populations of Golgi-derived vesicles, we have analyzed the distinct arrays of actin, myosins II, tropomyosin isoforms, and other proteins associ-

---

[1] The abbreviations used are: TGN, trans-Golgi network; mAb, monoclonal antibody; GTPγS, guanosine 5′-*O*-(3-thiotriphosphate); PAGE, polyacrylamide gel electrophoresis; JAS, Jasplakinolide.

Myosin Binding to Golgi Membranes

ated with different membrane domains. Probably through the actions of one or more of these proteins, newly budded vesicles have the ability to bind to actin filaments.

EXPERIMENTAL PROCEDURES

Antibodies—The monoclonal antibody (mAb) AD7, which recognizes p200/myosin II, has previously been characterized (4). Three antibodies were used to detect tropomyosin isoforms; the CG3 mAb raised against a peptide encoded by the TmNM5 gene (27) reacts with its Tm5NM-1, -2, -3, and -4 isoforms. A subset of these isoforms (Tm5NM-1 and 2) is more specifically recognized by the WS5/9d antibody raised against the product of the 9d exon (28). The polyclonal α_f9d antiserum recognizes Tms 2, 3, 5a, and 5b encoded by the αTm_{fast} gene and Tm1 from the β-Tm gene (29). The γ-adaptin antibody was a kind gift from Dr. M. S. Robinson (University of Cambridge, Cambridge, United Kingdom). mAbs against β-COP, an antibody against the 58-kDa peripheral Golgi protein, and α-smooth muscle actin were obtained from Sigma. Myosin IIA and IIB antibodies were a kind gift of Dr. R. S. Adelstein (National Institutes of Health, Bethesda, MD). The p23 antibody was provided by Dr. J. Gruenberg (University of Geneva, Geneva, Switzerland), the syntaxin 6 antibody by Dr. D. James (University of Queensland, Brisbane, Australia), and the Rab 6 antibody by Dr. B. Goud (Institute Curie, Paris, France). An antibody to rat dynamin I was from Transduction Laboratories (Lexington, KY). Secondary antibody conjugates were purchased from Vector Laboratories (Burlingame, CA).

Preparation of Golgi Membranes and Separation of Golgi-derived Vesicles—Golgi-rich membranes were prepared from rat liver homogenates using a procedure modified from Leelavathi *et al.* (30). Briefly, a post-nuclear supernatant of homogenized rat liver was layered onto a discontinuous sucrose gradient consisting of 2.5 ml of 1.3 M and 0.86 M sucrose solutions overlaid with 2 ml of 0.25 M sucrose. The gradients were centrifuged at 144,000 × g for 70 min. The supernatant of the 0.5 M sucrose layer was collected as cytosol, and the band above the 0.86 M sucrose interface was harvested as Golgi membranes. Snap-frozen cytosol and membrane samples were re-ultracentrifuged prior to use.

An *in vitro* assay for vesicle budding was used (31–33). Washed Golgi membranes (200 μg) were resuspended in HKM buffer (20 mM KCl, 2.5 mM magnesium acetate, 25 mM Hepes-KOH, pH 7.4) and preincubated with 0.1 mM GTPγS for 5 min at 37 °C, after which precleared cytosol (14 mg) was added and the reaction was continued for 30 min at 37 °C in the presence of 0.5 mM dithiothreitol and an ATP-regenerating system (4.6 IU/ml creatine phosphokinase, 81 mM creatine phosphate, and 28.6 mM ATP (disodium salt) in a 2-ml total volume). The reaction was terminated by incubation for 10 min in an ice-water slurry. The remnant (unbudded) Golgi cisternae were separated from the cytosol containing free vesicles by differential centrifugation (17,500 × g for 10 min at 4 °C). Vesicles were then separated from cytosol by discontinuous sucrose gradient centrifugation on 200 μl of 2.1 M sucrose, overlaid with 200 μl of 20% sucrose (w/w), and 2 ml of the cytosol/vesicle mixture (100,000 × g for 90 min at 4 °C). All sucrose solutions were prepared in HKM buffer. The cytosol was collected from the loading zone, and the budded vesicles were harvested at the 2.1 M/20% interface.

For vesicle separation, free vesicles were resuspended in a total volume of 400 μl of 20% sucrose and layered onto a discontinuous sucrose gradient consisting of 300 μl of each of the following sucrose solutions: 50%, 45%, 40%, 35%, 30%, and 25% (w/w) (33). The gradient was centrifuged for 18 h at 100,000 × g at 4 °C. The isopycnic gradient was fractionated from the bottom in 220-μl fractions by syringe puncture. Fractions were analyzed by SDS-PAGE and immunoblotting.

F-actin Binding Assay—Rat liver cytosol was precleared by ultracentrifugation (100,000 × g, 45 min, 4 °C), and aliquots (1 mg) were incubated in vesicle budding assay buffer (HKM buffer) supplemented with 0.5 mM dithiothreitol, 0.1 mM GTPγS, in the presence or absence of 5 mM MgATP at 37 °C for 45 min. Jasplakinolide (JAS, Molecular Probes, Eugene, OR) was added at a final concentration of 1 μM to polymerize/stabilize F-actin; we have shown previously that under these conditions cytosolic G-actin is efficiently converted to F-actin (20). F-actin was pelleted from the cytosol by low speed centrifugation (17,500 × g, 30 min, 4 °C), then washed in HKM buffer, and aliquots representing 100% of the F-actin pellet and 10% of the remaining cytosol supernatant were loaded onto SDS-PAGE gels and analyzed by immunoblotting to identify proteins coprecipitated with F-actin.

To analyze binding of Golgi vesicles to F-actin, vesicle fractions harvested from the vesicle separation gradient were diluted, ultracentrifuged (100,000 × g), and resuspended in HKM buffer. F-actin, polymerized with JAS from cytosol, was prepared in the presence of MgATP, to avoid saturation with soluble myosin II. Pelleted, washed F-actin was

resuspended and incubated with the vesicle fractions in the presence of GTPγS for 30 min at 37 °C. F-actin was then repelleted by centrifugation at low speed, and the resulting pellets and supernatants were analyzed by SDS-PAGE and immunoblotting to detect actin-bound vesicle-associated proteins and by electron microscopy to examine actin-bound vesicles.

SDS-PAGE and Immunoblotting—Samples for SDS-PAGE were separated on 5–15% gradient gels (34). Proteins were transferred onto Immobilon-P membrane in 15 mM Tris, 120 mM glycine, 20% methanol; membranes were routinely stained with 0.1% Coomassie Brilliant Blue R250 to check protein loading. For immunoblotting, transfers were blocked in Blotto (20 mM Tris, 150 mM NaCl, 5% skim milk, 1% Triton X-100), antibody incubations were carried out in Blotto for 1–2 h at room temperature or overnight at 4 °C, and bound antibodies were detected with alkaline phosphatase-conjugated secondary antibodies with 5-bromo-4-chloro-3-indolyl phosphate/nitro blue tetrazolium or with chemiluminescence.

Immunoelectron Microscopy—Golgi-enriched membranes and budded vesicles generated in the *in vitro* budding assay were fixed in 4% paraformaldehyde in phosphate-buffered saline overnight at 4 °C, collected on Formvar/carbon-coated copper grids by floating grids on 5-μl drops of suspensions of fixed budded membranes for 5 min at room temperature, then washed and stained with 1.8% methylcellulose containing 0.4% uranyl acetate for 10 min on ice. Negative contrast of whole mounts was obtained by staining with 1% uranyl acetate for 1 min and removal of excess stain with Whatman filter paper. Specimens were examined in a Joel 1010 transmission electron microscope.

Immunofluorescence Staining—NIH 3T3 fibroblasts grown at 8000 cells/cm^2 on poly-L-lysine substrate were serum-starved for 48 h, causing them to withdraw from the cell cycle into the G_0 (quiescent) phase of the cell cycle. Quiescent fibroblasts were fixed with 4% paraformaldehyde, permeabilized with chilled (-20 °C) methanol, and then double-immunostained with the WS5/9d antibody together with the 58K antibody that detects a peripheral Golgi membrane protein and the AD7 antibody. Goat anti-rabbit-conjugated lissamine rhodamine and goat anti-mouse-conjugated fluorescein secondary antibodies were used for detection. Staining patterns were analyzed by confocal scanning laser microscopy (Wild Leitz Instruments, Heidelberg, Germany).

RESULTS

Budding and Separation of Golgi-derived Vesicles—In vitro budding assays were performed using rat liver Golgi membranes and cytosol in the presence of GTPγS. Vesicle budding is demonstrated by the *de novo* membrane binding of two cytosolic proteins, p200/myosin II and β-COP (Fig. 1). Small amounts (<10%) of the coatomer protein β-COP and of p200/myosin II are present on freshly isolated, washed Golgi membranes (Fig. 1). Newly budded vesicles were initially separated from remnant cisternae and cytosol by centrifugation. The budded vesicle pellet is enriched in p200/myosin II and β-COP, compared with the original Golgi membranes, showing that coated vesicles have been generated during the assay and that these cytosolic proteins have specifically bound to them (Fig. 1). Some of the bound p200/myosin II and β-COP on the remnant Golgi cisternae (Fig. 1) represents attachment to additional budding sites or to budding vesicles that have not yet been released.

Golgi-derived vesicles were then separated on a second gradient, and fractions were analyzed by immunoblotting and densitometry to demonstrate the distribution of a range of vesicle-associated proteins (Fig. 2). The distributions of three proteins, p200/myosin II, β-COP, and γ-adaptin, were found to vary across the gradient (Fig. 2). Immunogold labeling has previously confirmed that β-COP (as part of the coatomer or COP I complex), γ-adaptin (a component of AP-1 clathrin-coated vesicles), and p200/myosin II are indeed localized on separate vesicles (5, 35). Thus the overlapping, but nevertheless distinct, peak distributions of p200/myosin II, β-COP, and γ-adaptin correspond to different populations of vesicles (Fig. 2). β-COP has a broader distribution throughout the gradient peaking at fractions F3–F7, and these same vesicles are labeled for p23, an integral membrane protein of coatomer-coated vesicles and the cis-Golgi-network (36–39) (Fig. 2A). γ-Adaptin
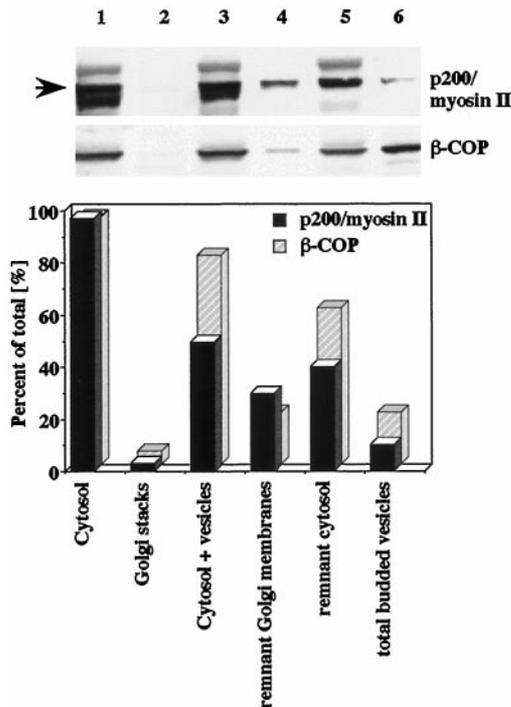
FIG. 1. **Cytosol and membrane fractions in the vesicle budding assay.** The budding reaction of Golgi-derived vesicles was monitored by immunoblotting for p200/myosin II and β-COP, present in the cytosol (*lane* 1) and in small amounts on isolated Golgi membranes (*lane* 2). After budding, both proteins are in a combined cytosol and vesicle fraction (*lane 3*) and some remained on remnant Golgi membranes (*lane 4*). Both proteins are found attached to vesicles (*lane 6*) after separation from remnant cytosol (*lane 5*). *Lanes 1*, *3*, and *5* represent 10% loading of each fraction while *lanes 2*, *4*, and *6* represent 100% of each pellet for one budding reaction. The *arrow* denotes the 200-kDa p200/myosin II band; a slower migrating band is sometimes recognized by the AD7 antibody (57). The *lower panel* shows the relative proportions of β-COP and p200/myosin II in various fractions. A large excess of both proteins is contributed by the cytosol, and ≤20% of both proteins is attached to budding vesicles.

FIG. 2. **Separation of Golgi-derived vesicles on sucrose density gradients.** *A*, vesicles from the budding reaction were separated by gradient centrifugation and immunoblotting detected p200, β-COP, p23, γ-adaptin, syntaxin 6, dynamin, Rab 6, Rab 4, and Rab 5 in fractions. The p200/myosin II and β-COP detected in F10 (loading zone) most likely represent small amounts of remaining cytosol. *B*, p200/myosin II, β-COP, and γ-adaptin define distinct sets of vesicles; peak distributions of each reveal the separation of three different vesicle populations.

peaks in fractions F4–F7, along with syntaxin 6, an integral membrane protein in TGN-derived clathrin-coated vesicles (40) (Fig. 2*A*). The peak distribution of p200/myosin II is in fractions F1–F5, but as yet there is no endogenous transmembrane marker with which to determine the identity of these vesicles. To ensure that the protein pattern reflects the distribution of membrane-bound proteins on vesicles in this gradient, the gradient was loaded with 1 mg of precleared cytosol and run under identical conditions. Soluble cytosolic proteins were found to distribute in fractions F8–F10 (data not shown); in these fractions, we are therefore unable to distinguish between vesicle-bound and soluble proteins (Figs. 2*A* and 3*B*). However, proteins in fractions F1–F7 were also analyzed on flotation gradients and were confirmed as being membrane-bound (data not shown). Thus, this gradient allows distinction and partial separation of three Golgi-derived vesicle populations demarked by the vesicle-associated proteins p200/myosin II, β-COP, and γ-adaptin.

Other vesicle-associated proteins were also detected on newly budded vesicles (Fig. 2*A*). Dynamin was distributed throughout the vesicle gradient and was not concentrated in any one vesicle population. The dynamin antibody used can recognize both dynamin I and dynamin II, and the two bands appearing in these gels could represent two isoforms or splice variants of dynamin. Rab 6, a monomeric G protein on Golgi membranes, was identified in fractions F3–F8, corresponding most closely to the distribution of β-COP labeled vesicles (Fig. 2*A*). Small amounts of Rab 4 were found in the gradient codis-

tributing with the peak γ-adaptin-labeled vesicles and barely detectable levels of Rab 5 were found in fractions toward the top of the gradient. While the bulk of vesicles on this gradient were generated from Golgi membranes, detection of these early endosome-associated Rabs indicates a very small contamination by plasma membrane/early endosome derived vesicles, possibly AP2 vesicles.

Actin and Actin-associated Proteins on Budded Vesicles— The gradient separation of vesicle populations provided a basis for analyzing the differential distribution of vesicle-associated cytoskeletal proteins. By immunoblotting, it was noted that β-actin was routinely present in fractions of Golgi membranes and vesicles (Fig. 3*A*). While most of the β-actin is found in the cytosol (Fig. 3, Table I), 7% of the β-actin present is on newly isolated stacked Golgi membranes. We routinely found that some of the total membrane-bound β-actin was lost to the cytosol during the budding assay, possibly due to dissociation or depolymerization of actin. However, some of the actin re-
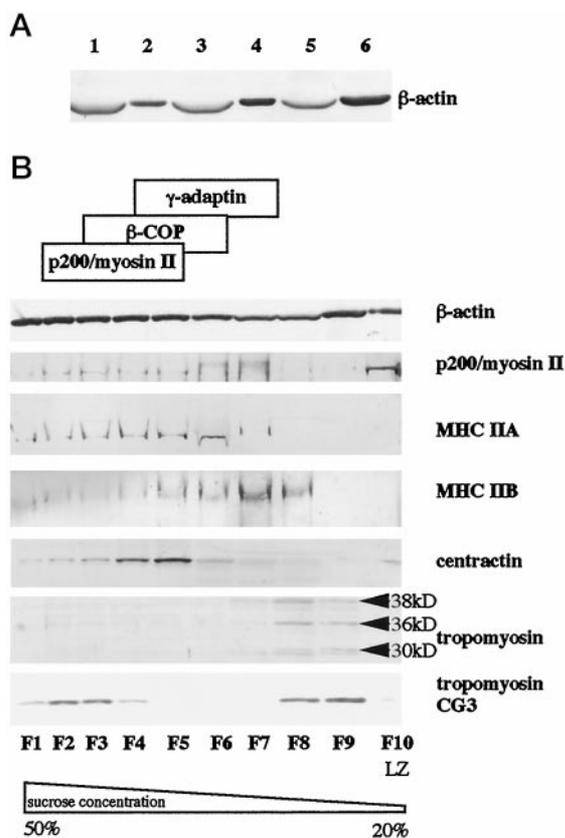
FIG. 3. **Distribution of actin and actin binding proteins.** *A*, β-actin was analyzed in fractions from the *in vitro* budding reaction by immunoblotting. *Lane 1*, cytosol; *lane 2,* isolated Golgi membrane; *lane 3*, cytosol containing the budded vesicles; *lane 4*, remnant Golgi cisternae; *lane 5*, remnant cytosol; *lane 6*, total budded vesicles. Total budded vesicles were separated from the remnant cytosol by ultracentrifugation on a sucrose step gradient. *B*, the distribution of actin and actin-binding proteins in the vesicle gradient was determined by immunoblotting. Actin distributes evenly across the gradient. p200/myosin II and myosin IIA are similarly in fractions F1–F5, while myosin IIB has a different distribution (F5–F8). Centractin peaks in F3–F6 along with β-COP. Tropomyosin isoforms recognized by the α_f9d antibody are clustered in fractions F8 and F9, most likely representing a cytosolic distribution. Tm5 tropomyosins recognized by CG3 are found in fractions containing cytosol (F8 and F9) and are also in a specific vesicle population (F1–F4).

TABLE I
Relative proportions of β-actin in assay fractions

A reproducible fraction of β-actin (7%) is bound to Golgi membranes in isolated Golgi stacks (G). Most of the β-actin in the assay is present in soluble form in the cytosol (C). Some of the membrane-bound β-actin is present in total budded vesicles (P2, 3%) or remains on Golgi cisternae (P1). The amounts of β-actin in SDS-PAGE gel fractions were analyzed by immunoblotting and densitometry. These data are representative of three experiments. S1, cytosol + vesicles; S2, remnant cytosol.

Fractions	C	G	S1	P1	S2	P2
Total β-actin (%)	93	7	99	≤1	96	3

mains bound to remnant cisternae and a consistent proportion (3% of total) of the β-actin binds to the budded vesicles (Fig. 3, Table I). β-Actin bound to all populations of vesicles and was evenly distributed across all of the fractions of the vesicle gradient (Fig. 3*B*). Each vesicle fraction contained approximately 0.3% of the total vesicle-associated β-actin. Centractin was detected at low levels throughout the gradient but was particularly concentrated in the β-COP-labeled vesicle population (Fig. 3*B*), suggesting that it does bind preferentially to these vesicles. p200/myosin II, which has been identified as nonmuscle myosin IIA, is found on one of the TGN-derived

vesicle populations, and immunoblotting with an antibody raised against the heavy chain of nonmuscle myosin IIA shows a similar distribution peaking in fractions F1–F5, as expected. In contrast, the nonmuscle myosin IIB isoform has a different distribution, peaking in fractions F6–F8. The distribution of membrane-bound myosin IIB overlaps with that of γ-adaptin vesicles, while some of the myosin IIB, in the higher fractions, may also be cytosolic (Fig. 3*B*). These results now show that more than one population of Golgi-derived vesicles is associated with a member of the myosin II family and that myosin II isoforms are targeted separately to specific vesicle-budding membrane domains.

Tropomyosin isoforms were analyzed on Golgi membranes and budded vesicles using two antibodies. Blotting with the α_f9d antibody shows several low and high molecular mass (30–38 kDa) isoforms of the αTm_{fast} and β-TM gene families in fractions at the top of the gradient, which may represent the presence of cytosolic proteins (Fig. 3*B*). We found no evidence for αTm_{fast} and β-TM tropomyosins binding to Golgi membranes before budding (data not shown) or to newly budded vesicles (Fig. 3*B*). Probing with an antibody (CG3) that sees all isoforms of the Tm5 gene family reveals a single band, which could represent more than one isoform, and this was present in both Golgi membrane and cytosol fractions. On the vesicle gradient, the Tm5 band is seen in fractions at the top of the gradient (F8–F9) which are likely to represent cytosolic Tm5, and in fractions F1–F4, clearly representing Tm5 bound to selected vesicles. Tm5 in these lower fractions of the gradient coincides with the distribution of p200/myosin II-labeled vesicle population (Fig. 3*B*).

In order to further investigate whether p200/myosin II and Tm5 are colocalized on the same vesicles, or are on different populations of co-migrating vesicles, immunostaining was carried out with the AD7 antibody to p200/myosin II and with an antibody (WS5/9d) that recognizes a subset of Tm5 gene products. Fig. 4 shows a quiescent 3T3 fibroblast labeled with the 58K antibody and the WS5/9d antiserum. Two isoforms (Tm5NM-1 and -2) co-localize identically with the 58K Golgi peripheral membrane protein in an asymmetric perinuclear fashion. However, fibroblasts double-stained with p200/myosin II (Fig. 4*C*) and WS5/9d (Fig. 4*D*) showed intense but mutually exclusive perinuclear staining patterns, suggesting that Tm5 isoforms and p200/myosin II are enriched in different compartments of the Golgi complex (Fig. 4, *C* and *D*, *arrows*). Comparison of p200/myosin II staining with TGN38 showed that both proteins colocalized and were enriched in the TGN (Fig. 4, *E* and *F*, respectively). This suggests that at least some of the Tm5 isoforms recognized by CG3 in the liver Golgi fractions are on separate vesicles from p200/myosin II. These observations demonstrate an actin-based structural complexity of the Golgi-derived vesicle network, and suggest that specific microfilament populations may have unique roles to play in Golgi function.

Interaction of Actin-based Motor Proteins with F-actin—The presence of actin and actin-binding proteins on Golgi-derived vesicles led us to investigate whether individual vesicle-associated proteins and the vesicles themselves could bind to actin filaments (Figs. 5 and 6). Rat liver cytosol (100,000 $\times$ *g* supernatant) contained mostly G-actin, which was not pelleted by low speed centrifugation (Fig. 5). When rat liver cytosol was incubated with the actin-polymerizing drug JAS, 50% of the total actin, detected with a general actin antibody, formed F-actin, which could be pelleted at low speed. This F-actin was then incubated with cytosol or with the newly budded vesicle fractions to test the actin-binding properties of soluble proteins (Fig. 5) and vesicles (Fig. 6), respectively. As an actin-based
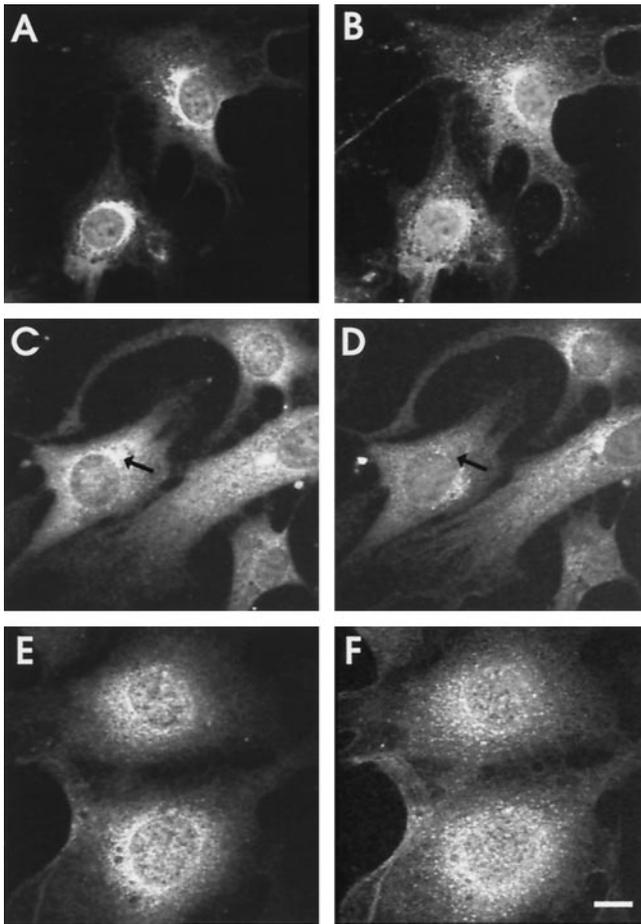
FIG. 4. **Tm5NM-1 and -2 do not colocalize with p200/myosin II in fibroblasts.** Quiescent NIH 3T3 fibroblasts were double-labeled by immunofluorescence with antibodies to p200/myosin II, Tm5 isoforms, and Golgi markers and analyzed by confocal microscopy. The staining comparisons shown are within the same optical section. *Panels A* and *B*, cells labeled with the 58K protein antibody and the WS5/9d antibody, respectively, show identical Golgi staining. *Panels C* and *D*, cells stained with the AD7 antibody and the WS5/9d antibody, respectively, show different staining patterns in the Golgi area. *Panels E* and *F*, cells stained with antibodies to p200/myosin II as TGN38, respectively, show the same staining over the TGN and analyzed by confocal microscopy. Thus, Tm5NM-1 and -2, recognized by the WS5/9d antibody, colocalize with the 58K protein but not with p200/myosin II in the Golgi region.
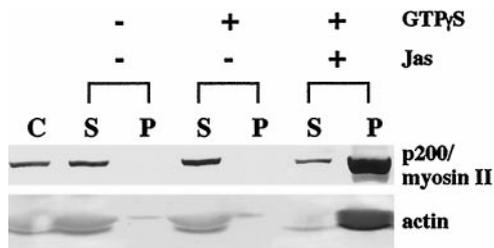
FIG. 5. **Binding of p200/myosin II to F-actin.** Figure shows p200/myosin II and actin in fractions of cytosol (*C*). Cytosol was incubated with or without GTPγS and JAS as indicated; resulting F-actin was recovered by low speed centrifugation, and the actin pellets (*P*) and supernatants (*S*) were analyzed by immunoblotting. p200/myosin II is in the supernatants and is only co-sedimented with F-actin produced by JAS (*P*). *S*, supernatant, 10% loading of total fraction on gel; *P*, pellet, 100% loading on gel.

motor, p200/myosin II in the cytosol would be expected to bind to actin filaments; accordingly, we found that 50% of the soluble p200/myosin II in the cytosol was pelleted along with the F-actin, under these conditions (Fig. 5). In control experiments, neither the incubation buffer nor the addition of GTPγS to the
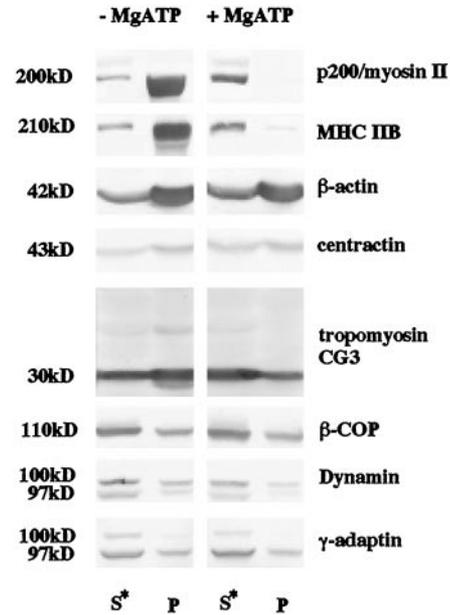
FIG. 6. **Binding of cytosolic proteins to F-actin.** Cytosol was incubated with JAS in the presence and absence of MgATP. Pelleted F-actin (*P*) and supernatants (*S*) were analyzed by immunoblotting. Motor proteins (p200/myosin II and myosin IIB), centractin, β-actin, and tropomyosin show significant amounts of sediment with F-actin (*P*) whereas only insignificant amounts of β-COP, γ-adaptin, and dynamin pelleted with F-actin. The actin binding of p200/myosin II and myosin IIB is dramatically reduced in the presence of MgATP. *S**, supernatant, 10% of total fraction loaded on gel; *P*, pellet, 100% loading.

cytosol was sufficient to induce polymerization of F-actin or pelleting of p200/myosin II (Fig. 5). This assay was also carried out in the presence and absence of MgATP, which typically dissociates motor proteins from actin (Fig. 6). While 50% of p200/myosin II and myosin IIB bound to F-actin in the absence of MgATP, both myosins II were liberated upon treatment with MgATP, no longer appearing in the F-actin pellet (Fig. 6). These data confirm that both p200/myosin II (myosin IIA) and myosin IIB in the cytosol can associate with F-actin via their head domains. In contrast, centractin (30%) was pelleted with F-actin in a MgATP-independent fashion (Fig. 6). Tm5 tropomyosins also bound to F-actin in this assay, and this binding was slightly reduced in the presence of MgATP (Fig. 6).

As controls, we also tested whether other cytosolic, vesicle-associated proteins, which are not known to bind actin, could be pelleted with F-actin. Soluble forms of β-COP and γ-adaptin did not pellet in significant amounts in either the presence or absence of MgATP and therefore did not bind specifically to F-actin (Fig. 6). We also found that, under these conditions, cytosolic dynamin, in its GTP-bound form in the presence of GTPγS, did not bind appreciably to F-actin (Fig. 6).

Golgi-derived Vesicle Populations Associate with F-actin— Having confirmed that some of the vesicle-associated proteins have the ability to bind to F-actin, we next investigated whether intact, newly budded vesicles themselves could bind to F-actin (Figs. 7 and 8). Actin was polymerized with JAS from rat liver cytosol, in the presence of MgATP to avoid saturation of F-actin with soluble motors such as p200/myosin II, and the F-actin was then pelleted at low speed (Fig. 7, *P1*). Vesicles were collected from separated fractions of the vesicle separation gradient. In order to initially collect vesicles, the sucrose concentration was reduced, but this did not release any of the membrane-bound β-COP or p200/myosin II (Fig. 7, *S2*). The vesicles were resuspended and incubated with cytosol containing F-actin in the presence of GTPγS (to avoid loss of vesicle coats) in the absence of MgATP, and F-actin was then pelleted

Myosin Binding to Golgi Membranes

p200/myosin II

S1 P1 S2 P2 S P S P
              F2   F3

β-COP

S1 P1 S2 P2 S P S P
              F4   F5
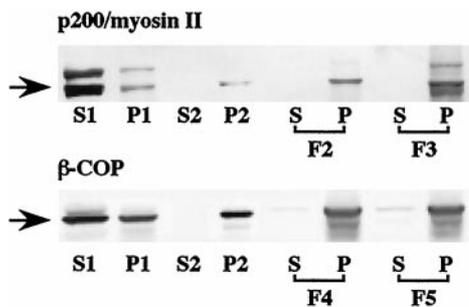
FIG. 7. **Golgi-derived vesicles bind to F-actin.** Actin polymerized from rat liver cytosol with JAS in the presence of MgATP shows little binding of either soluble p200/myosin II or β-COP (*P1*). More than 90% of these soluble proteins remain in the supernatant (*S1*; 10% loading) upon pelleting F-actin by differential centrifugation (*P1*; see Fig. 6). More than 90% of both proteins remain in the supernatants (*S1*; see Fig. 6 for loading details). Golgi-derived vesicle fractions (F2–F3, p200 vesicles; and F4–F5, β-COP vesicles) from the sucrose density gradient were diluted and recovered by ultracentrifugation. The resulting supernatant (*S2*) and pellet (*P2*) show that p200/myosin II and β-COP remain bound to the vesicles after resuspension. Resuspended fractions across the gradient were incubated with F-actin; the F-actin was then recovered by low speed centrifugation (*P*). Under these conditions, both p200/myosin II and β-COP vesicles pelleted with F-actin. Small amounts of β-COP remain in the supernatant (*S*). *S*, supernatant, 10% loading of total fraction on gel; *P*, pellet, 100% loading.

at low speed under conditions that did not pellet vesicles alone. Nearly all of the vesicles in fractions collected from the p200/myosin II peak and the β-COP peak bound to the F-actin. Small amounts of β-COP in the supernatant could be due to saturation of F-actin binding for these vesicles or due to some uncoating of vesicles. In order to confirm that intact vesicles bind to F-actin, the pelleted vesicles were also examined by electron microscopy. Different types of intact, coated vesicles were identified in the budded vesicle fraction (Fig. 8, *A–C*). Coated vesicles and vesicle profiles were found in the F-actin pellet (Fig. 8*D*), and some vesicle profiles can be seen bound to actin filaments (Fig. 8, *D* and *E*). Negative contrast of the F-actin/vesicle pellet reveals superpolymerized F-actin (Fig. 8*F*, *arrows*) as well as normal F-actin (Fig. 8*F*, *arrowheads*) around vesicles. Taken together, these data show that newly budded Golgi-derived vesicles can bind to F-actin, presumably through the interaction of one or more of the actin-binding proteins present on each vesicle population.

DISCUSSION

The budding assay described in this paper yields multiple populations of intact, coated vesicles derived from Golgi membranes (Fig. 9). When the full complement of vesicles was further separated by gradient centrifugation, three distinct populations were harvested and identified by the presence of the vesicle-associated proteins p200/myosin II, β-COP, and γ-adaptin as markers. Each of these proteins from the cytosol bound to Golgi membranes in a GTP-dependent fashion during the budding assay, and each was then recovered in distinct peak fractions of the vesicle separation gradient. The separation of these vesicles is consistent with results obtained by immunoelectron microscopy showing that β-COP and p200/myosin II (5) and γ-adaptin and p200/myosin II (35) are on separate populations of Golgi-derived vesicles. In addition, there are undoubtedly other types of Golgi-derived vesicles present. For instance, β-COP has also been found on non-clathrin-coated vesicles budding off other parts of the Golgi complex, including the TGN (41). Two other types of vesicles that bud off the TGN are potentially also present within this gradient: vesicles labeled with the p230 protein, which are distinct from those bearing p200/myosin II (42); and those defined by the AP-3 adaptor complex, which bud off the TGN

for transit to late endosomes and lysosomes (43). Our data also suggest that fractions F1–F4 on the gradient contain separate populations of vesicles labeled for either p200/myosin II or for Tm5 isoforms.

Other proteins were found on one or more populations of vesicles. The Rab family of monomeric G proteins bind to different classes of transport vesicles and commonly serve as compartment markers. Rab 6 was found to codistribute with β-COP, consistent with it being on vesicles involved in trafficking in early parts of the Golgi stack, most likely those involved in retrograde transport (44). Dynamin is a GTPase implicated in the scission of clathrin-coated vesicles at the plasma membrane (45, 46). Dynamin II has been localized on the TGN, where it appears to be involved in the budding of at least two vesicle populations: clathrin-coated vesicles and constitutive secretory vesicles labeled for pIgA-R (47). Our data similarly indicate a GTP-dependent binding of dynamin II to Golgi membranes and additionally show that dynamin is distributed across the whole gradient and is therefore associated with multiple populations of vesicles and that dynamin does stay attached to the membranes on newly budded vesicles after their release. The presence of dynamin on all budded vesicles suggests that it may form part of a generalized budding machinery, perhaps by aiding vesicle interactions with both microtubules and microfilaments, through binding to profilin and amphiphysin (48, 49).

A dedicated spectrin/ankyrin network is assembled on Golgi membranes (16, 18) and, although the functions of this network are not yet understood, it has potential roles in maintaining Golgi structure, in marshaling transmembrane proteins within the plane of Golgi membranes and/or in vesicular transport (50). Based on the equivalent spectrin structure at the plasma membrane, it is reasonable to assume that short actin filaments or actin-like molecules are also associated with the Golgi complex. Centractin (ARP1) is an actin-related protein shown to associate with spectrin on plasma membranes and on Golgi membranes (51). Our data show that centractin is on newly budded vesicles and, unlike actin itself, it is concentrated on COP I vesicles. As part of the dynactin complex (52), centractin has the potential to link Golgi membranes or vesicles with microtubules. COP I vesicles are known to associate with microtubules (53) and have recently been shown to associate with spectrin/ankyrin (50), suggesting several possible roles for centractin on these vesicles. Our results also indicate that small amounts of actin itself, as the β-actin isoform (<10%), is stably associated with Golgi membranes and that some β-actin is bound to budded vesicles. Unlike the other vesicle-associated proteins, β-actin was slightly de-enriched in the budded vesicle fraction compared with the Golgi stack, suggesting that relatively more of the actin is retained on non-budding membrane domains of Golgi cisternae. In addition, β-actin was present on all newly budded vesicles and, when tested, vesicles from all fractions appeared to be equally competent to bind to F-actin. The presence of membrane-associated actin with both the Golgi cisternae and with budding vesicles suggests that actin filaments could be both a structural component of the Golgi stack as well as participating in trafficking. By electron microscopy, under normal conditions of the budding reaction, we did not observe prominent actin filaments associated with budded vesicles. Polymerized actin produced in the presence of JAS could, however, be seen associated directly with vesicles. Thus, actin present on Golgi membranes and/or on vesicles under physiological conditions may be composed primarily of short filaments, or actin filaments may associate with the membranes only transiently. Actin on budded vesicles could be transferred from the donor Golgi membranes, or new short filaments could

FIG. 8. **Golgi-derived vesicles and F-actin-bound vesicles.** Vesicles budded from rat liver Golgi membranes (Fig. 1, *lane 6*) and Golgi-derived vesicles bound to F-actin were examined as whole mounts by transmission electron microscopy. The total vesicle population contains coated vesicles of distinct appearance and size (*A–C*). Vesicles with typical clathrin coats (*A* and *B*) and smaller coats (*C*) were recognized. Intact coated vesicles (*arrowhead*) were recovered in the F-actin pellet (*D*). Actin filaments (*arrows*) could be seen in these samples, often aligned with vesicles (*D* and *E*). Negative contrast of whole mounts reveals the association of different lipid vesicles with fine actin filaments (*arrowheads*) as well as with long, superpolymerized F-actin (*arrows*, *F*). *Scale bar*, 200 nm.
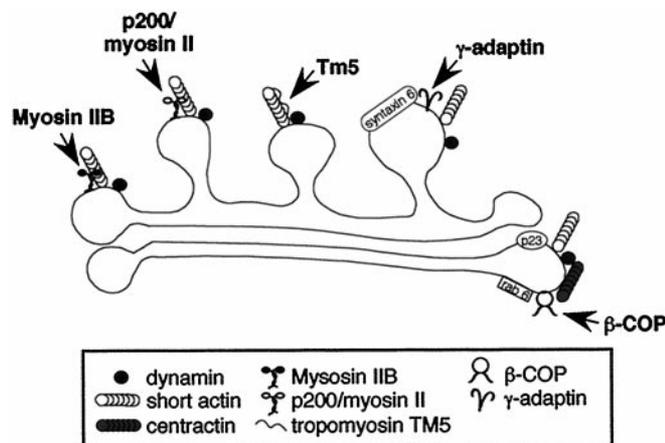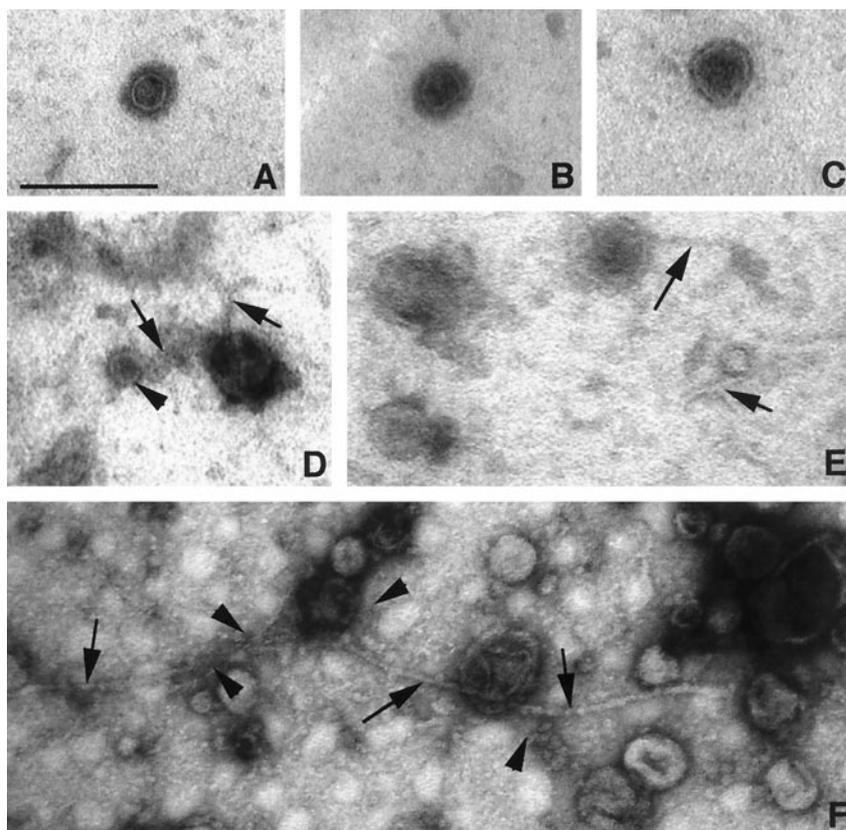
FIG. 9. **Schematic summary of cytoskeletal proteins associated with different vesicles.** Different Golgi-derived vesicle populations, depicted as budding profiles, are distinguished by the presence of different cytoskeletal proteins and vesicle markers. F-actin is associated with all newly budded vesicles. Myosins IIA and B, and Tm5 are, however, found on distinct vesicles consistent with there being customized or unique actin filaments on different vesicle populations. It has been shown that coating actin with different Tm isoforms has the demonstrated potential to influence the specificity of their interaction with different myosin isoforms (61).

arise from local nucleation sites on the surface of vesicles.

Tropomyosins associate closely with actin filaments and serve to regulate filament stability and length. Cells typically express several types and isoforms of tropomyosins, and there is growing evidence to show that specific isoforms can be differentially localized on actin filaments throughout cells (54). Tropomyosins of the Tm5 family, recognized by the CG3 antibody, were detected here on rat liver Golgi membranes and were on at least one specific vesicle population. This correlates well with the demonstration that Tm5NM-1 and Tm5NM-2 isoforms of the Tm5 family are localized on Golgi membranes in

fibroblasts, as shown by immunofluorescence. In contrast, tropomyosins detected by the $\alpha_f 9d$ antibody, were not found on vesicles. These findings indicate that tropomyosin isoforms mark specific populations of microfilaments associated with discrete cellular subcompartments. It also provides compelling evidence that these different filament populations have specific cellular functions (55). Actin filament heterogeneity may be regulated throughout cells and even within the Golgi milieu by the differential placement of tropomyosins associated with membranes and vesicles. One of the two tropomyosin isoforms in *S. cerevisiae* has been implicated in post-Golgi trafficking (56) by the finding that temperature-sensitive mutants of the *TPM1* gene accumulate Golgi-derived transport vesicles. A functional interaction of tropomyosin with a myosin V in this pathway is further suggested, since the *TPM1* gene shows synthetic lethality with the *MYO2* gene (56). An important role of tropomyosins in vesicle trafficking could potentially be to liaise with myosin motors in coordinating filament stability and vesicle movement.

Myosins of multiple families appear in association with Golgi membranes and on newly budded vesicles in cells (1, 35). p200/myosin II is homologous to the heavy chain of non-muscle myosin IIA (MHCIIA) and is on a specific subset of TGN-derived vesicles (35, 57). It is interesting to note that non-muscle myosin IIB is on different Golgi-derived vesicles. In several cell types, nonmuscle myosins IIA and IIB have been found on distinct membrane domains and have been ascribed to different cellular functions such as cytokinesis and cell motility (58, 59). The current data, however, provide the first indication that both non-muscle myosin II isoforms could be involved in trafficking and that there is highly specific targeting of each protein to distinct vesicle-budding domains of Golgi membranes. Myosin I is also found on vesicles budding off Golgi membranes, where it is proposed to provide motor activity for vesicle movement along actin filaments at the cell periphery (10). The non-muscle myosins IIA and B, both in the cytosol

and on vesicles, are oriented for actin binding in a MgATP-dependent motor-like configuration. p200/myosin II binds to the vesicles in a GTP-dependent fashion during budding, and it dissociates from vesicles soon after budding,[2] suggesting it may function only in the locale of the Golgi. However, there are conflicting reports about whether p200/myosin II is an essential participant in the vesicle budding reaction (6, 60). Thus, as with actin/membrane interfaces in other parts of the cell, the surfaces of Golgi-derived vesicles appear to harbor multiple classes of motors, perhaps for a series of temporal interactions with microfilaments. Possible mechanisms for binding vesicles to actin filaments, and their associated proteins, include direct binding via myosins I or II or indirect association of actin with the vesicle surface through spectrin/ankyrin assemblies. Membrane binding through any of the known mechanisms for vesicle-associated proteins, for instance through different actions of ARF-GTP (50), is likely to result in dynamic or temporary binding of microfilaments to vesicles.

These data add to the emerging evidence that the Golgi complex is associated with the actin cytoskeleton through multiple families of actin-binding proteins or actin-based motors. Moreover, we show that specific isoforms or members of these families are placed strategically and specifically on specific membrane domains, or on specific vesicle populations. The binding of specific isoforms of Tm5 tropomyosins to selected vesicles suggests a mechanism for customizing actin filament stability during vesicle budding or trafficking. Isoforms of myosin II on different vesicles could also provide for different motor activity, vesicle movement, or attachment to actin filaments during budding. A key issue to now resolve is how individual actin-binding proteins and actin filaments bind to vesicles and the relationships of these proteins during budding or subsequent trafficking.

REFERENCES

1. Fath, K. R., Trimbur, G. M., and Burgess, D. R. (1994) *J. Cell Biol.* **126,** 661–675
2. Stow, J. L., Fath, K. R., and Burgess, D. R. (1998) *Trends Cell Biol.* **8,** 138–141
3. Burkhardt, J. K. (1998) *Biochim. Biophys. Acta* **1404,** 113–126
4. Narula, N., McMorrow, I., Plopper, G., Doherty, J., Matlin, K. S., Burke, B., and Stow, J. L. (1992) *J. Cell Biol.* **117,** 27–38
5. Narula, N., and Stow, J. L. (1995) *Proc. Natl. Acad. Sci. U. S. A.* **92,** 2874–2878
6. Müsch, A., Cohen, D., and Rodriguez-Boulan, E. (1997) *J. Cell Biol.* **138,** 291–306
7. Ikonen, E., Parton, R. G., Lafont, F., and Simons, K. (1996) *Mol. Biol. Cell* **7,** 961–974
8. Poucell-Hatton, S., Perkins, P. S., Deerinck, T. J., Ellisman, M. H., Hardison, W. G., and Pandol, S. J. (1997) *Gastroenterology* **113,** 649–658
9. Montes de Oca, G., Lezama, R. A., Mondragon, R., Castillo, A. M., and I., M. (1997) *Arch. Med. Res.* **28,** 321–328
10. Fath, K. R., and Burgess, D. R. (1993) *J. Cell Biol.* **120,** 117–127
11. Fath, K. R., Trimbur, G. M., and Burgess, D. R. (1997) *J. Cell Biol.* **139,** 1169–1181
12. Evans, L. L., Hammer, J., and Bridgman, P. C. (1997) *J. Cell Sci.* **110,** 439–449
13. Prekeres, R., and Terrian, D. M. (1997) *J. Cell Biol.* **137,** 1589–1601
14. Mermall, V., Post, P. L., and Mooseker, M. S. (1998) *Science* **279,** 527–533
15. Echard, A., Jollivet, F., Martinez, O., Lacapere, J. J., Rousselet, A., Janoueix-Lerosey, I., and Goud, B. (1998) *Science* **279,** 580–585
16. Beck, K. A., Buchanan, J. A., Malhotra, V., and Nelson, W. J. (1994) *J. Cell Biol.* **127,** 707–723
17. Devarajan, P., Stabach, P. R., Mann, A. S., Ardito, T., Kashgarian, M., and Morrow, J. S. (1996) *J. Cell Biol.* **133,** 819–830
18. Beck, K. A., Buchanan, J. A., and Nelson, W. J. (1997) *J. Cell Sci.* **110,** 1239–1249
19. Heuser, J. (1989) *Cell Biol. Int. Rep.* **13,** 1063–1076
20. Shurety, W., Stewart, N. L., and Stow, J. L. (1998) *Mol. Biol. Cell* **9,** 957–975
21. Santos, B., and Snyder, M. (1997) *J. Cell Biol.* **136,** 95–110
22. Walch-Solimena, C., Collins, R. N., and Novick, P. J. (1997) *J. Cell Biol.* **137,** 1495–1509
23. Johnston, G. C., Prendergast, J. A., and Singer, R. A. (1991) *J. Cell Biol.* **113,** 539–551
24. Hill, K. L., Catlett, N. L., and Weisman, L. S. (1996) *J. Cell Biol.* **135,** 1535–1549
25. Govindan, B., Bowser, R., and Novick, P. (1995) *J. Cell Biol.* **128,** 1055–1068
26. Mulholland, J., Wesp, A., Riezman, H., and Botstein, D. (1997) *Mol. Biol. Cell* **8,** 1481–1499
27. Novy, R. E., Sellers, J. R., Liu, L.-F., and Lin, J. J.-L. (1993) *Cell Motil. Cytoskel.* **25,** 267–281
28. Weinberger, R., Schevzov, G., Jeffrey, P., Gordon, K., Hill, M., and Gunning, P. (1996) *J. Neurosci.* **16,** 238–252
29. Schevzov, G., Lloyd, C., and Gunning, P. (1992) *J. Cell Biol.* **117,** 775–785
30. Leelavathi, D. E., Estes, I. W., Feingold, D. S., and Lombardi, B. (1970) *Biochim. Biophys. Acta* **211,** 124–138
31. de Almeida, J. B., Doherty, J., Ausiello, D. A., and Stow, J. L. (1993) *J. Cell Sci.* **106,** 1239–1248
32. Serafini, T., Stenbeck, G., Brecht, A., Lottspeich, F., Orci, L., Rothman, J. E., and Wieland, F. T. (1991) *Nature* **349,** 215–220
33. Serafini, T., and Rothman, J. E. (1992) *Methods Enzymol.* **219,** 286–299
34. Laemmli, U. K. (1970) *Nature* **227,** 680–685
35. Stow, J. L., and Heimann, K. (1998) *Biochim. Biophys. Acta* **1404,** 161–171
36. Nickel, W., Sohn, K., Bunning, C., and Wieland, F. T. (1997) *Proc. Natl. Acad. Sci. U. S. A.* **94,** 11393–11398
37. Rojo, M., Pepperkok, R., Emery, G., Kellner, R., Stang, E., Parton, R. G., and Gruenberg, J. (1997) *J. Cell Biol.* **139,** 1119–1135
38. Sohn, K., Orci, L., Ravazzola, M., Amherdt, M., Bremser, M., Lottspeich, F., Fiedler, K., Helms, J. B., and Wieland, F. T. (1996) *J. Cell Biol.* **135,** 1239–1248
39. Tang, B. L., Wong, S. H., Qi, X. L., Low, S. H., and Hong, W. (1993) *J. Cell Biol.* **120,** 325–328
40. Bock, J. B., Lin, R. C., and Scheller, R. H. (1996) *J. Biol. Chem.* **271,** 17961–17965
41. Griffiths, G., Pepperkok, R., Locker, J. K., and Kreis, T. E. (1995) *J. Cell Sci.* **108,** 2839–2856
42. Gleeson, P. A., Anderson, T. A., Stow, J. L., Griffith, G., Toh, B. H., and Matheson, F. (1996) *J. Cell Sci.* **109,** 2811–2821
43. Odorizzi, G., Cowles, C. R., and Emr, S. D. (1998) *Trends Cell Biol.* **8,** 282–288
44. Martinez, O., and Goud, b. (1998) *Biochim. Biophys. Acta* **1404,** 101–112
45. Shpetner, H. S., Herskovits, J. S., and Vallee, R. B. (1996) *J. Biol. Chem.* **271,** 13–16
46. Damke, H., Baba, T., Warnock, D. E., and Schmid, S. L. (1994) *J. Cell Biol.* **127,** 915–934
47. Jones, S. M., Howell, K. E., Henley, J. R., Cao, H., and McNiven, M. A. (1998) *Science* **279,** 573–577
48. Witke, W., Podtelejnikov, A. V., Di Nardo, A., Sutherland, J. D., Gurniak, C. B., Dotti, C., and Mann, M. (1998) *EMBO J.* **17,** 967–976
49. Owen, D. J., Wigge, P., Vallis, Y., Moore, J. D., Evans, P. R., and McMahon, H. T. (1998) *EMBO J.* **17,** 5273–5285
50. De Matteis, M. A., and Morrow, J. S. (1998) *Curr. Opin. Cell Biol.* **10,** 542–549
51. Holleran, E. A., Tokito, M. K., Karki, S., and Holzbauer, E. L. (1996) *J. Cell Biol.* **135,** 1815–1829
52. Clark, S. W., Staub, O., Clark, I. B., Holzbauer, E. L., Paschal, B. M., Vallee, R. B., and Meyer, D. I. (1994) *Mol. Biol. Cell* **5,** 1301–1310
53. Lowe, M., and Kreis, T. E. (1998) *Biochim. Biophys. Acta* **1404,** 53–66
54. Gunning, P., Weinberger, R., and Jeffrey, P. (1997) *Anat. Embryol.* **195,** 311–315
55. Gunning, P., Weinberger, R., Jeffrey, P., and Hardeman, E. (1998) *Annu. Rev. Cell Dev. Biol.* **14,** 339–372
56. Liu, H., and Bretscher, A. (1992) *J. Cell Biol.* **118,** 285–299
57. Ikonen, E., de Almeida, J. B., Fath, K. R., Burgess, D. R., Ashman, K., Simons, K., and Stow, J. L. (1997) *J. Cell Sci.* **110,** 2155–2164
58. Kelley, C. A., Sellers, J. R., Gard, D. L., Bui, D., Adelstein, R. S., and Baines, I. C. (1996) *J. Cell Biol.* **134,** 675–687
59. Maupin, P., Phillips, C. L., Adelstein, R. S., and Pollard, T. D. (1994) *J. Cell Sci.* **107,** 3077–3090
60. Simon, J.-P., Shen, T.-H., Ivanov, I. E., Gravotta, D., Morimoto, T., Adesnik, M., and Sabatini, D. D. (1998) *Proc. Natl. Acad. Sci. U. S. A.* **95,** 1073–1078
61. Fanning, A. S., Wolenski, J. S., Mooseker, M. S., and Izant, J. G. (1994) *Cell Motil. Cytoskel.* **29,** 29–45

---

[2] K. Heimann and J. L. Stow, unpublished observations.

Specific Isoforms of Actin-binding Proteins on Distinct Populations of Golgi-derived Vesicles

Kirsten Heimann, Justin M. Percival, Ron Weinberger, Peter Gunning and Jennifer L. Stow

Access the most updated version of this article at http://www.jbc.org/content/274/16/10743

Alerts:
- When this article is cited
- When a correction for this article is posted

Click here to choose from all of JBC's e-mail alerts

This article cites 61 references, 43 of which can be accessed free at
http://www.jbc.org/content/274/16/10743.full.html#ref-list-1